Experimental Neurology 321 (2019) 113037

Contents lists available at ScienceDirect

Experimental Neurology

journal homepage: www.elsevier.com/locate/yexnr

Research paper

Enhanced regeneration and reinnervation following timed GDNF gene therapy in a cervical ventral root avulsion

Ruben Eggers[a,*], Fred de Winter[a], Cleo Arkenaar[a], Martijn R. Tannemaat[a,b], Joost Verhaagen[a,c]

[a] Laboratory for Neuroregeneration, Netherlands Institute for Neuroscience, An institute of the Royal Academy of Arts and Sciences, Amsterdam, The Netherlands
[b] Department of Neurology, Leiden University Medical Center, Leiden, The Netherlands
[c] Department of Molecular and Cellular Neurobiology, Center for Neurogenomics and Cognition research, Vrije Universiteit Amsterdam, Amsterdam, The Netherlands

ARTICLE INFO

Keywords:
Root avulsion
Brachial plexus
Gene therapy
GDNF
Nerve injury
Regeneration

ABSTRACT

Avulsion of spinal nerve roots is a severe proximal peripheral nerve lesion. Despite neurosurgical repair, recovery of function in human patients is disappointing, because spinal motor neurons degenerate progressively, axons grow slowly and the distal Schwann cells which are instrumental to supporting axon extension lose their pro-regenerative properties. We have recently shown that timed GDNF gene therapy (dox-i-GDNF) in a lumbar plexus injury model promotes axon regeneration and improves electrophysiological recovery but fails to stimulate voluntary hind paw function. Here we report that dox-i-GDNF treatment following avulsion and reimplantation of cervical ventral roots leads to sustained motoneuron survival and recovery of voluntary function. These improvements were associated with a twofold increase in motor axon regeneration and enhanced reinnervation of the hand musculature. In this cervical model the distal hand muscles are located 6,5 cm from the reimplantation site, whereas following a lumber lesion this distance is twice as long. Since the first signs of muscle reinnervation are observed 6 weeks after the lesion, this suggests that regenerating axons reached the hand musculature before a critical state of chronic denervation has developed. These results demonstrate that the beneficial effects of timed GDNF-gene therapy are more robust following spinal nerve avulsion lesions that allow reinnervation of target muscles within a relatively short time window after the lesion. This study is an important step in demonstrating the potential of timed GDNF-gene therapy to enhance axon regeneration after neurosurgical repair of a severe proximal nerve lesion.

1. Introduction

A severe brachial plexus injury leads to a complete loss of function of the arm, severely affecting the patient's quality of life. Despite neurosurgical repair strategies to restore anatomical continuity between the injured motor axons and the distal nerves, recovery of function of the distal musculature is often disappointing (Shin et al., 2005; Kachramanoglou et al., 2017). In patients with a brachial plexus injury, axons need to regenerate distances of up to 80 cm before reaching their distal target muscles in the lower arm and hand. With an average axonal outgrowth velocity of 1–2 mm/day, axon regeneration is a protracted process, which takes many months and even years.

During the first weeks after a nerve injury, substantial axonal regeneration occurs due to a pro-regenerative response in the injured neurons and the denervated Schwann cells in the distal nerve stump. Axotomized spinal motoneurons upregulate a set of regeneration-associated genes and shift from a stable transmitting to a regenerative state (Piehl et al., 1998; Mason et al., 2003; Abe and Cavalli, 2008; Risling et al., 2011). In the peripheral nerve stump distal to the lesion, Schwann cells convert into repair cells (Jessen and Mirsky, 2002; Arthur-Farraj et al., 2012; Jessen and Mirsky, 2016; Arthur-Farraj et al., 2017). The repair Schwann cells form the bands of Bungner and are specialized to promote axon regeneration. Important pro-regenerative molecular features of the repair Schwann cell include the upregulation of cell-adhesion molecules, cytokines and neurotrophic factors. In the rat, these cellular and molecular changes are sufficient to support axon regeneration for a post-lesion time period of 6 to 8 weeks (Giannini and Dyck, 1990; Fu and Gordon, 1995; Sulaiman and Gordon, 2000; Hoke et al., 2002). In most rodent models, nerve injury and repair occurs close to the target musculature. In these situations, axons have to grow

Abbreviations: AV, Avulsion; ChAT, Choline acetyl transferase; CMAP, Compound muscle action potential; dox, Doxycycline; dox-i-GDNF, Doxycycline inducible GDNF vector system; GDNF, Glial cell line-derived neurotrophic factor; GArrtTA, Glycine alanine repeat sequence fused to reverse tetracycline controlled transactivator; LV, Lentivirus

* Corresponding author at: Netherlands Institute for Neuroscience, Meibergdreef 47, Amsterdam 1105 BA, The Netherlands.
E-mail address: r.eggers@nin.knaw.nl (R. Eggers).

https://doi.org/10.1016/j.expneurol.2019.113037
Received 14 June 2019; Received in revised form 1 August 2019; Accepted 14 August 2019
Available online 16 August 2019

over relatively short distances resulting in substantial axonal regeneration and recovery of function. However, during prolonged regeneration periods, chronic axotomy and denervation progressively impairs axonal regeneration. In chronically axotomized motoneurons, a decline in regeneration-associated gene expression occurs after 4 weeks (Tetzlaff et al., 1991; Sulaiman and Gordon, 2013; Gordon and Tetzlaff, 2015). In the distal nerve, the chronically denervated Schwann cells start to lose their pro-regenerative phenotype after 4 weeks with the loss of neurotrophic factor expression, endoneurial tube fibrosis and fragmentation of the Schwann cell basal lamina (Giannini and Dyck, 1990; Funakoshi et al., 1993; Hoke et al., 2002; Eggers et al., 2010; Brushart et al., 2013). The failure of motoneurons and Schwann cells to support axon regeneration beyond a critical period of 6 to 8 weeks explains the observation that following proximal lesions, which require much longer regeneration periods, distal muscle reinnervation and recovery of function is poor (Fu and Gordon, 1995; Hoke et al., 2002; Eggers et al., 2010; Sulaiman and Gordon, 2018).

Avulsion of the lumbar ventral nerve roots from the spinal cord is the most severe proximal peripheral nerve lesion possible. Axotomy close to the motoneuron cell body results in progressive motoneuron death (Koliatsos et al., 1994; Bergerot et al., 2004; Penas et al., 2009; Eggers et al., 2010). Reimplantation of avulsed ventral roots temporarily delays motoneuron degeneration and allows staggered regeneration of motor axons over the implantation site into the nerve root (Eggers et al., 2010; Romeo-Guitart et al., 2017). However, following lumbar ventral root avulsion regenerating axons have to grow 10 to 13 cm to reach their target muscles in the hind paw. To bridge this distance an extended period of regeneration is required, resulting in limited distal regeneration and recovery of voluntary function does not occur (Eggers et al., 2010; Torres-Espin et al., 2013). To promote motoneuron survival and long distance axonal regeneration, we recently studied the effect of timed GDNF gene therapy in the reimplanted lumbar ventral roots using a novel immune-evasive gene switch (Eggers et al., 2019). Time-restricted GDNF expression enhanced motoneuron survival and stimulated long distance axonal regeneration about 2-fold. Although these were encouraging results, electromyographical analysis demonstrated that the first signs of reinnervation of the most distal musculature in GDNF treated animals occurs at 12 weeks post implantation, whereas voluntary functional recovery was not observed in control as well as GDNF treated animals (Eggers et al., 2019). These observations suggest that GDNF gene therapy in lumbar ventral roots could not overcome the detrimental effects of chronic nerve denervation that occurs following this severe proximal lesion.

In this study we investigated the effect of timed GDNF gene therapy on axon regeneration following avulsion of cervical ventral roots. In the rat, the distal intrinsic hand musculature is located approximately 6,5 cm from the cervical spinal avulsion and reimplantation site. Therefore, following a cervical lesion axons have to regenerate approximately half the distance compared to our previous study on GDNF gene therapy in a lumbar plexus lesion (Eggers et al., 2019). Due to the reduction in the regeneration distance, the Schwann cells in the nerve will not develop a severe state of chronic denervation but will retain a certain capacity to support axon regeneration. Our results demonstrate that following cervical ventral root avulsion and reimplantation a limited degree of functional recovery of the denervated forepaw occurs in untreated rats. Timed GDNF gene therapy in the reimplanted ventral roots promoted motoneuron survival, stimulated distal axonal outgrowth, target muscle reinnervation and recovery of voluntary forepaw function. In contrast to the lack of voluntary functional recovery of the hind paw after a lumbar plexus injury (Eggers et al., 2019), timed GDNF gene therapy promoted recovery of function of the forepaw after cervical plexus injury. In conclusion, the current results demonstrate that the beneficial effects of timed GDNF-gene therapy are more robust following spinal nerve avulsion lesions that allow target reinnervation within a relatively short time window after the lesion.

2. Methods

2.1. Production of lentiviral vectors

Second-generation lentiviral (LV) vectors were produced using a 3 plasmid co-transfection [the VSV-G envelope protein vector (pMD.G.2), the viral core packaging vector (pCMVdeltaR8.7.4) and the transfer vector plasmid (pLV-CMV-GArGFP, pLV-TRE-GDNF or pLV-CMV-GArrtTA)] in Human embryonic kidney 293 T (HEK293T) cells as described previously (Naldini et al., 1996; Hendriks et al., 2007; Eggers et al., 2019). LV particles were harvested from the medium by ultracentrifugation and dissolved in phosphate buffered saline (pH 7.4). LV stocks were titered by infecting HEK293T cells with serial dilutions of the LV stocks (Hoyng et al. 2014). After 48 h genomic DNA of the transduced cells was extracted and viral integration was quantified by PCR using primers directed against the WPRE and a SYBR green PCR kit (Applied Biosystems). The titer in transgene expressing units (TU)/ml was calculated based on a standard curve generated with an LV-GFP stock run in parallel with the experimental LV stocks. LV vectors used in this study were control vector LV-CMV-GArGFP (CMV-GFP negative control; 2.0×10^{10} GC/ml), LV-TRE-GDNF (1.10×10^{10} GC/ml) and LV-CMV-GArrtTA (5.6×10^{10} GC/ml). The TRE-GDNF and CMV-GArrtTA vector stocks were mixed and utilized in a 1:1 ratio and referred to as dox-i-GDNF.

2.2. Study design and surgical procedures

Young adult female Wistar rats ($n = 37$, 180–200 g Charles River, Germany) were housed under standard conditions at a 12:12 h light/dark cycle with ad libitum access to water and regular- or doxycycline (dox) supplemented chow (6 g doxycycline/kg chow, TD.09282, Envigo). All animal procedures were approved by the local laboratory animal welfare committee and are in accordance with European guidelines (86\609\EEC). Animals and intervention groups were randomized over the cages. The investigators performing the functional and histological assessments were blind to the intervention groups.

Rats were assigned to one of three intervention groups (Fig. 1D), including an avulsion-only negative control group (AV-only; $n = 10$), a CMV-GArGFP control group (CMV-GFP; $n = 12$) and a timed dox-i-GDNF intervention group (a 1:1 mixture of TRE-GDNF and CMV-GArrtTA; $n = 15$). A hemilaminectomy and opening of the dura was performed under general isoflurane anaesthesia (Isoflo, Abbott, the Netherlands). In all animals, the C7 and C8 dorsal root ganglia were removed to allow for lentiviral vector injection into the ventral root and reimplantation of the injected root into the spinal cord. The motoneurons innervating the distal flexor muscles responsible for generating grip strength, are located in the C6, C7, C8 and T1 spinal segments and project an axon towards the median, ulnar and radial nerve (Bertelli et al., 1995; McKenna et al., 2000; Tosolini and Morris, 2012). To fully denervate the hand musculature and establish complete electrophysiological function loss, an unilateral avulsion of ventral roots C6, C7, C8 and T1 was performed directly at the surface of the spinal cord. Careful visual inspection confirmed complete avulsion of all four rootlets. In the AV-only group no reimplantation was performed and distal roots were trimmed away to prevent reinnervation. In both CMV-GFP and dox-i-GDNF groups the C7 and C8 ventral roots were injected with 1 µl of viral vector each (Fig. 1B, C) using a glass needle as described previously (Eggers et al., 2008). Fast green was added to the viral vector solution to monitor the injection procedure (FCF, Sigma). The roots were implanted into their corresponding spinal cord segment at a depth of 0.5 mm and fixed in place using fibrin glue (TissueCol; Baxter B.V.). Analgesia was obtained by per-operative Temgesic injection (Buprenorphine 0.03 ml/100 g body weight s.c., Schering-Plough B.V.). Animals were kept warm until full recovery from anaesthesia.

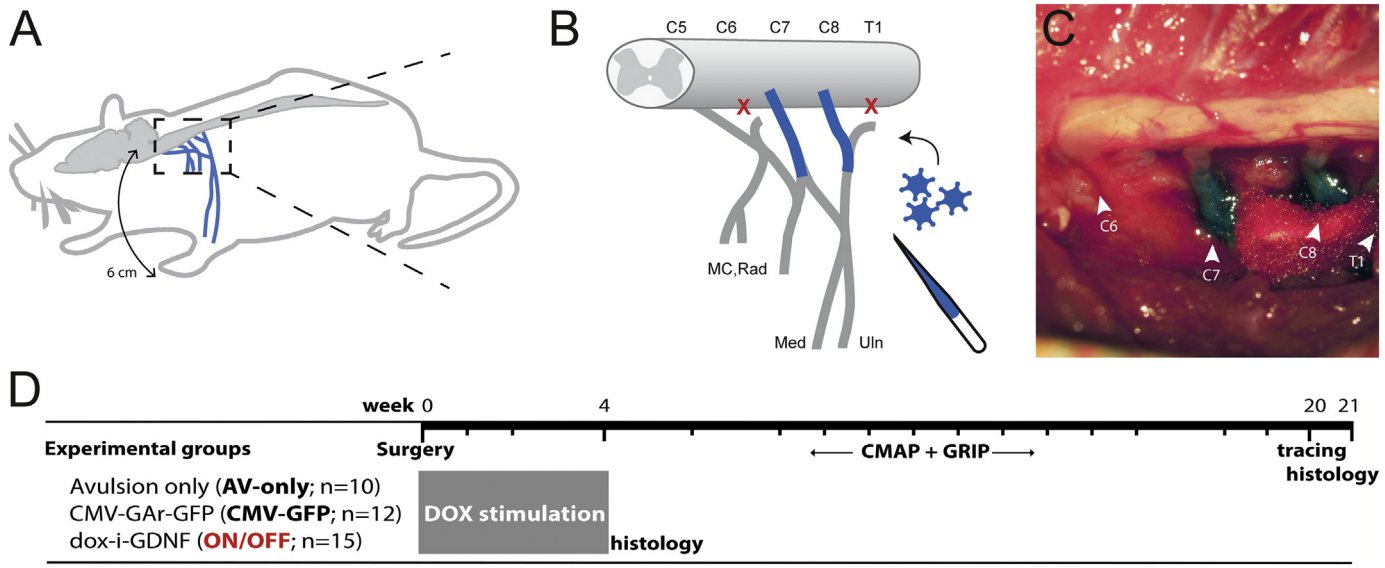

Fig. 1. Surgical procedures and experimental design. (A–B) Schematic overview of the brachial plexus and peripheral nerves innervating the rat forepaw. (B) Schematic outline of the surgical procedures. Avulsion of C6 to T1 ventral roots followed by a LV-vector injection into the avulsed C7 and C8 ventral roots and reimplantation into the ventro-lateral aspect of the spinal cord. (C) Picture of the avulsed and reimplanted C7-8 ventral roots following injection of the LV-vector. The addition of fast green to the viral vector solution assists in visualizing the ventral root injection. (D) Experimental design detailing the experimental groups, number of animals per group, duration of dox application (4 weeks, in grey) and timing of retrograde tracing at 20 weeks and endpoint histology (21 weeks). The compound muscle action potentials (CMAPs) were recorded prior to the surgery and every second week starting at post-lesion week 1. (MC; musculocutaneous, Rad; radial, Med; median, Uln; ulnary). (For interpretation of the references to colour in this figure legend, the reader is referred to the web version of this article.)

2.3. Doxycycline food supplementation

Directly following surgery, all rats received dox supplemented food (6 g/kg) for a period of 4 weeks post-surgery (Fig. 1D), after which they returned to regular chow. The 4 week time period is based on four previous observations. First, we found that 8 weeks of GDNF expression leads to axonal entrapment, while at four weeks this was not yet observed (Eggers et al., 2008). Second, although within the first week the first regenerating axons have entered the reimplanted ventral root, the majority of axons enter the roots between weeks 2 and 4 weeks (Eggers et al., 2010). Third, motoneurons become increasingly unresponsive to reimplantation or GDNF treatment beyond the critical period of 4 to 6 weeks post avulsion (Chai et al., 1999; Zhou and Wu, 2006). Finally, a treatment period of 4 weeks is sufficient to exert long-lasting neuroprotective effects on motoneurons (Eggers et al., 2019).

2.4. Assessment of compound muscle action potential

To monitor the timing and degree of reinnervation, compound muscle action potential (CMAP) were recorded from the intrinsic palmar musculature under isoflurane anaesthesia by an observer blinded to the treatment. A supramaximal percutaneous 0.1 ms stimulus was applied using an electromyograph (Dantec Keypoint) and a custom made bipolar electrode with an interelectrode spacing of 1,5 mm. The stimulus was applied medial to the cubital fossa, stimulating the ulnar and median nerve. The intrinsic hand muscle CMAPs were recorded using a needle electrode placed at the pollex in the volar aspect of the hand. The signal was referenced to an electrode placed subcutaneously at the dorsum of the third digit. CMAP measurements were performed preoperative and at one week postoperative to confirm completeness of the avulsion lesion. The first two months CMAP amplitude recordings were performed every 2 weeks, followed by weekly recordings up to week 20.

2.5. Assessment of forepaw grip strength

Recovery of voluntary flexor muscle strength of the forepaw was measured using a grip strength apparatus (TSE systems, Germany). Prior to surgery, animals were pretrained to familiarize them to the handling procedure. The contralateral forepaw was manually reflected backwards while the animals were advanced towards a horizontal sensor bar. After gripping the bar, animals were gently pulled backwards with a constant speed until grip was no longer maintained and the maximum grip strength was recorded. A minimum of three measurements per animal were performed and averaged for each time point. If an animal was unable to grip the bar and generate a recording, a zero score was assigned. Measurements were rejected if the contralateral paw touched the sensor. Grip strength recordings were performed every two weeks.

2.6. Retrograde motoneuron labelling

To quantify the number of motoneurons that regenerated an axon into the intrinsic hand musculature located 6,5 cm distal from the implantation sites, all animals were subjected to retrograde tracing 20 weeks after surgery (Fig. 1D). Under isofluane anaesthesia, two 1 µl 4% Fluoro Gold (FG) injections (Fluorochrome, LLC; USA) were performed by inserting the 30G needle of a 10 µl Hamilton syringe to a depth of 5 mm at the hypothenar aspect of the hand. Animals were sacrificed 5 days post-tracing to allow sufficient retrograde tracer transport to the spinal motoneurons.

2.7. Tissue preparation

At 4 weeks post-implantation, three dox-i-GDNF treated animals were perfused and the brachial plexus dissected to assess GDNF expression during dox supplementation. At 21 weeks post-surgery, all remaining animals were anesthetized using sodium pentobarbital and transcardially perfused with cold saline followed by 4% paraformaldehyde (PFA) in PBS. Cervical C5-T2 spinal cord segment was post-fixed in PFA for 2 h and incubated in 250 mM EDTA in PBS overnight to soften residual bone debris. The brachial plexus was dissected between the spinal column and axilla. The medial and ulnar nerves were dissected between the cubital fossa up to 5 mm proximal.

All tissues were cryoprotected in 25% sucrose for 2 days at 4 °C prior to mounting in OCT Compound and snap-frozen in dry ice cooled 2-methylbutane. Four series of longitudinal spinal cord sections were cut on a cryostat at a thickness of 25 µm and mounted on Superfrost Plus slides (Menzel-Gläser, Braunsweig, Germany). Longitudinal brachial plexus and transverse medial and ulnar nerve sections were cut in three series at a thickness of 20 µm. Intrinsic hand musculature sections were cut at 40 µm thickness and mounted in a drop of 50 mM EDTA on Superfrost Plus slides. All sections were stored at −80 °C until further processing.

2.8. Staining procedures and histological evaluation

Longitudinal spinal cord and transverse median and ulnar nerve sections were subjected to an immunohistochemical staining for choline acetyl transferase (ChAT) to visualize motoneurons and their axons. Briefly, sections were incubated overnight in 10 mM citrate buffer (pH 6.0) at room temperature followed by incubation in blocking buffer (PBS containing 5% FCS and 0.3% Triton X-100). Subsequently, sections were incubated overnight in blocking buffer containing primary antibody directed against ChAT (1:200 Ab-144P Chemicon) followed by incubation with a biotinylated secondary antibody (1:200; anti-goat Biotin; Jackson). Subsequent incubation with avidin-biotin-peroxidase complex (ABC; 1:800 PK-6100 Elite Vectastain ABC kit, Vector laboratories), allowed final staining development using 0.035% 3′ 3′-diaminobenzamidine tetrahydrochloride (DAB) in TBS containing 0.01% H_2O_2 and 0.2 mg/ml $(NH_4)_2.SO_4.NiSO_4$.

Longitudinal sections of the brachial plexus and palmar musculature were subjected to immunofluorescence staining following a standard staining protocol as described previously (Eggers et al., 2019). To visualize GFP, endogenous GDNF and vector-derived GDNF expression in the brachial plexus, all sections were incubated overnight at 4 °C in blocking buffer containing primary antibodies directed against GFP (1:400, MAB3580 Merck Millipore), GDNF (1:500, AF212NA, R&D systems) and Tubulin-β3 (1:400, MMS-435P Biolegend). Incubation was followed by 2 h incubations with secondary antibodies anti-Chicken Alexa-488, anti-mouse Alexa-594 (1:800), Biotinylated anti-goat (1:200) and Streptavidin Cy3 (Jackson ImmunoResearch). Quantification of the number of GFP positive cells was performed in longitudinal brachial plexus sections of CMV-GFP injected animals. High resolution images were made with a Leica SP5 confocal microscope and analysed using Fiji software. GFP positive nuclei were discriminated from the background by creating a mask using a threshold between 30 and 255, followed by an automated particle analysis. Subsequently, the number of GFP positive nuclei per mm nerve length was determined and averaged.

Neuromuscular junctions (NMJ) of the palmar musculature were stained using primary antibodies directed against Tubulin-β3 (1:400, MMS-435P Biolegend) and synaptic vesicle protein SV2 (1:200, SV2 DSHB) to visualize the presynaptic nerve terminals and Biotin-conjugated α-Bungarotoxin (1:500, B1196 Molecular Probes) to stain for postsynaptic acetylcholine receptors AChRs. After overnight binding at 4 °C, sections were incubated with the appropriate secondary antibody in blocking buffer for 2 h (anti-Mouse Alexa-488 (1:800); Streptavidin Cy5 (1:400); Jackson ImmunoResearch). All sections were embedded in 10% Mowiol, 2,5% Dabco in TrisHCl.

2.9. Motoneuron quantification

Manual quantification of the number of retrogradely traced FG positive motoneurons present in the C5-T2 spinal cord segments was performed directly after sectioning without embedding in mounting medium in every fourth section. Using a fluorescence microscope (Zeiss), excitation at 365 nm resulted in specific white FG positive motoneurons. Subsequently, these spinal cord sections were stained for ChAT to quantify the total number of surviving motoneurons. As described previously (Eggers et al., 2019), ChAT positive motoneurons present in the ventral motoneuron pool and containing a nucleus were included in the quantification. The number of ipsilateral and contralateral motoneurons was manually quantified and the percentage of surviving motoneurons for each animal was calculated. In these ChAT stained sections, motoneuron soma surface area was manually quantified in 4 animals per group. High-resolution images of the C7-C8 ventral motoneuron pool were made using a Zeiss brightfield microscope. ChAT positive motoneuron profiles of the ipsilateral side were manually outlined using Fiji software and the surface area per neuron was determined. Per treatment group, the average surface area was subsequently expressed as a percentage of intact controls.

2.10. Peripheral nerve axon quantification

Assessment of the number of regenerating axons was performed in transverse ChAT stained median and ulnar nerve sections 38 mm distal from the implantation site. An observer blind to the treatment groups performed a manual quantification of the total number of motor axons. To aid in the quantification, custom-made Image Pro Plus-based (MediaCybernetics, USA) software was used to outline the two nerve fascicles at a low magnification. Subsequently, a digital counting grid was placed covering the outlines in which the total number of ChAT positive fibers was counted at high magnification.

2.11. Muscle innervation and endplate formation

The percentage of innervated NMJs was quantified in palmar muscle sections stained for AChRs (Fig. 7; red) and axon terminals (green). *Z*-stack images were collected with a Leica SP5 confocal microscope and collapsed into a single image. Three sections per animal were randomly selected and the endplate band was photographed. Based upon the pre- and postsynaptic staining, endplates were scored as denervated or innervated. Partial or full overlap between nerve terminals and the AChR cluster was scored as innervated, whereas no overlap was scored as a denervated endplate. Partially visible NMJs that were not positioned in parallel to the imaging plane were excluded and an average of 80 NMJs were analysed per animal.

2.12. Animal exclusion and statistical analysis

During surgical procedures, one animal from the AV-only and one animal from the dox-i-GDNF was lost. An assessment of complete distal musculature denervation was performed after avulsion. Based upon the presence of a small CMAP response at 7 days post-lesion, two animals (one animal from the AV-only and one animal from the dox-i-GDNF group) were excluded from all further analysis. The final experimental groups contained the following number of animals: AV-only ($n = 8$), CMV-GFP ($n = 12$), dox-i-GDNF ($n = 10$). Data were expressed as mean ± SEM. Differences with $p < 0.05$ was considered statistically significant. Analysis was performed using Prism (Graphpad software, Inc.). A normality test (Shapiro-Wilk) was followed by one-tailed student's *t*-test to determine statistical significance. Time dependent data were analysed using two-way ANOVA for repeated measures followed by post-hoc Bonferroni. Simple linear regression analysis was performed to examine predictive relationships between variables.

3. Results

3.1. GFP and GDNF transgene expression in the reimplanted ventral root and brachial plexus

To assess the lentiviral vector-mediated transduction of the reimplanted cervical ventral roots, longitudinal sections of the brachial plexus of all animals at either 4 ($n = 3$) or 21 ($n = 30$) weeks post-surgery were all stained for GFP, GDNF and Tubulin-β3 to visualize transgene expression and axon regeneration (Fig. 2). In intact spinal

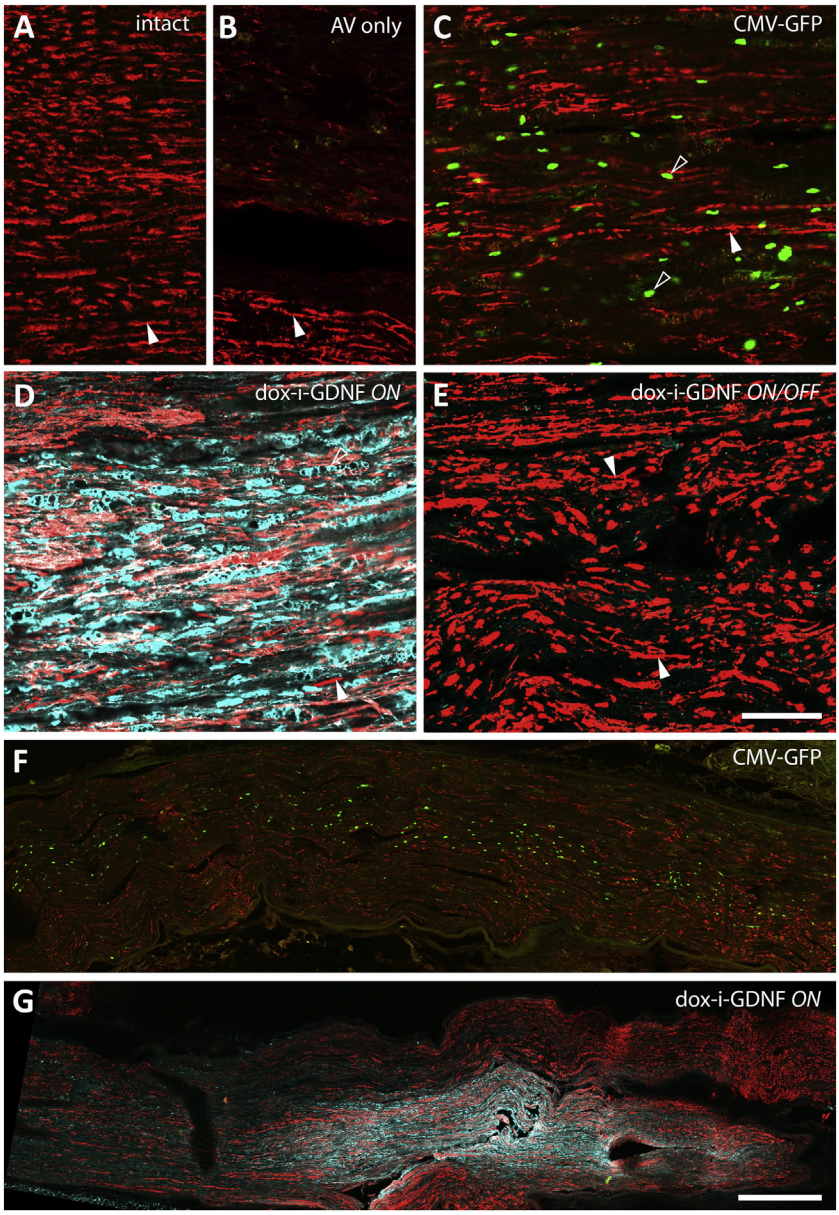

Fig. 2. Regulation of GDNF protein expression and distribution of transduced cells. (A–G) Representative images of GDNF and GFP protein expression in longitudinal brachial plexus sections 4 and 21 weeks post-lesion (All sections were stained for GDNF; cyan, GFP; green, tubulin-β3; red). (A–B) Compared to intact cervical nerves, nerve roots in the AV-only animals do not contain axons due to motor axon loss. Axons from intact adjacent dorsal root ganglia remained present (arrowhead). (C) Reimplantation of control CMV-GFP injected ventral roots enables small diameter regenerating motor axons to regenerate into the brachial plexus (arrowhead). Nuclear GFP staining confirms persistent GFP expression in the brachial plexus up to 21 weeks post implantation (open arrowhead), whereas no GDNF staining was observed. (D) **In** dox-i-GDNF treated animals during dox supplementation at 4 weeks, immunofluorescence staining for GDNF protein reveals intracellular and secreted GDNF (cyan). **(E)** At 21 weeks, in dox-i-GDNF treated animals the levels of GDNF are comparable to those observed in the CMV-GFP sections, confirming that the expression of GDNF was switched off**.** Fibers grow in a longitudinal orientation and no local axon entrapment or axon coil formation was observed. (F, G) In low magnification images, spread of CMV-GFP and dox-i-GDNF transduced cells over a distance of 5 mm can be appreciated. Scale bar in D (A–D) = 30 μm; E = 500 μm. (For interpretation of the references to colour in this figure legend, the reader is referred to the web version of this article.)

roots nerve fascicles containing well-organized large diameter axons were observed (Fig. 2A). As expected, in the AV-only group a clear loss of axons had occurred (Fig. 2B). The remaining large diameter axons in the AV-only group are most likely sensory axons originating from the adjacent C5, 6 or T1 dorsal root ganglia. In contrast, lesioned and reimplanted ventral roots injected with the control vector CMV-GFP exhibited many small diameter regenerating motor axons that had crossed the implantation site into the brachial plexus (Fig. 2C). Immunofluorescence staining for GFP protein confirms persistent GFP expression in the brachial plexus up to 21 weeks post implantation, whereas no GDNF staining was observed. Large numbers of GFP positive nuclei of transduced cells (329 ± 33 nuclei/ mm nerve length) are evenly distributed throughout the nerves (Fig. 2C, F). Assessment of the most distally transduced cells shows that viral injection into the ventral root transduced cells in the brachial plexus up to 5 mm distally from the implantation site. In the dox-i-GDNF treated animals during dox supplementation at 4 weeks, immunofluorescence staining for GDNF protein reveals the presence of intracellular and secreted GDNF (Fig. 2D, G). Although we cannot exclude that some endoneurial fibroblasts have been transduced, the majority of GDNF positive cells have the classical elongated morphology of denervated Schwann cells. At 21 weeks, in dox-i-GDNF treated animals the levels of GDNF staining are comparable to those observed in the CMV-GFP sections, confirming the expression was switched off (Fig. 2C, E). In both CMV-GFP and dox-i-GDNF groups, the number of small diameter regenerating fibers appear similar and grow in a longitudinal orientation. No local axon entrapment or axon coil formation was observed. These observations show that LV vectors transduce a substantial number of cells and the dox-i-GDNF gene switch significantly enhances the expression of GDNF in the reimplanted nerve roots during the first 4 weeks after the lesion.

3.2. Dox-i-GDNF treatment combined with reimplantation improves voluntary grip strength compared to reimplantation only

To investigate whether timed GDNF expression leads to improved reinnervation and recovery of function, electrophysiological CMAP and grip strength analysis was performed during the 20 week regeneration period. Despite the avulsion of all 4 ventral roots (C6, C7, C8 and T1) that supply the the distal flexor muscles via the median, ulnar and radial nerve, a small CMAP response was detected at 7 days post-injury in

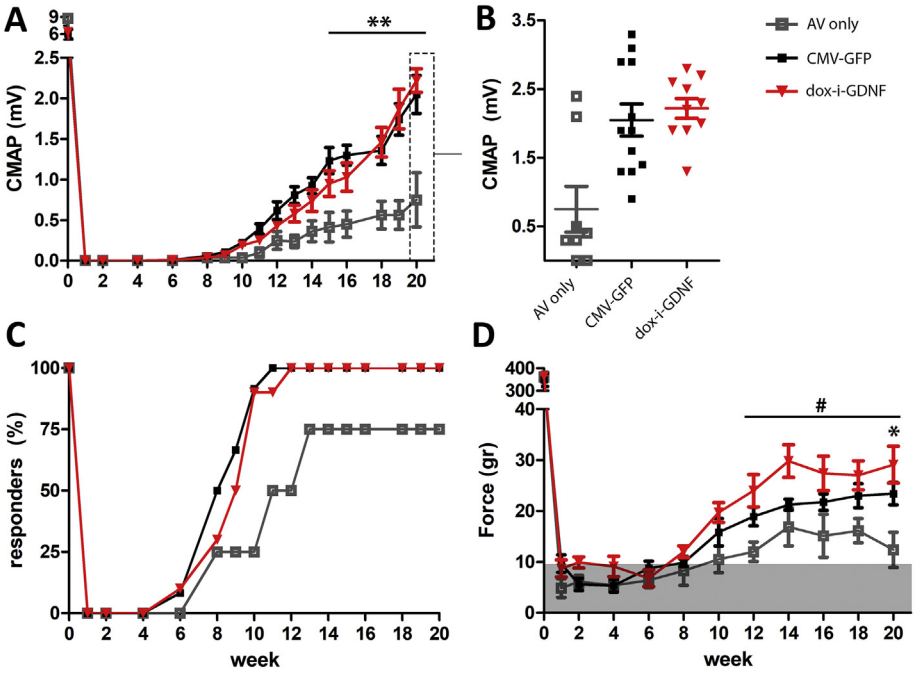

Fig. 3. Reimplantation combined with timed GDNF expression improves voluntary grip strength but does not lead to improved CMAP function. (A–C) Compound muscle action potentials (CMAP) were recorded in the intrinsic palm musculature during a 20 week recovery period. (A) Compared to AV-only, gradual CMAP amplitude increase in both re-implanted groups result in significant difference after 15 weeks. (B) CMAPs of individual animals at 20 weeks (boxed area in A) to further detail inter-group variation. (C) The first CMAP responses in reimplanted CMV-GFP and dox-i-GDNF treated animals occurred at 6 weeks, contrasting a 2 week delay in AV-only animals. (D) Ventral root reimplantation results in increasing voluntary grip strength starting between 8 and 10 weeks in CMV-GFP and dox-i-GDNF groups. No significant difference exists between AV-only and CMV-GFP up to 20 weeks. In contrast, dox-i-GNDF treatment results in early and significant improvement compared to AV-only. Grey area in D represents background values generated without gripping the bar. (A) ** $p < 0.001$ versus AV. (D) # $p < 0.01$ dox-i-GDNF versus AV-only. *p < 0.01 CMV-GFP versus AV-only. Data represent mean ± SEM.

two animals. These animals were excluded from further analysis. In the AV-only group, CMAP responses remained completely absent in 25% of the animals during the 20 week monitoring period. Starting at 8 weeks, in some AV-only animals low CMAP responses were observed which remained low throughout the post-lesion observation period of 20 weeks (0.75 ± 0.33 mV; Fig. 3A-C). At week 6 the first animals in both CMV-GFP and dox-i-GDNF groups displayed a small CMAP response (Fig. 3C). During the subsequent 5 weeks, the number of animals with a CMAP response increased to 100% in both groups. A progressive increase in CMAP amplitudes in both CMV-GFP and dox-i-GDNF treated groups resulted in significantly higher amplitudes compared to AV-only ($p < 0.001$). No difference between CMV-GFP and dox-i-GDNF was found with groups reaching amplitudes of 2.05 ± 0.23 mV or 2.22 ± 0.15 mV respectively at 20 weeks (Fig. 3B).

In agreement with the CMAP results, voluntary function distal from the elbow was lost directly post-lesion as animals were unable to grip the bar. During the first 5 weeks of testing, in all animals low grip strength values were observed, which were primarily due to brushing of the animal's forepaw perpendicular to the bar (Fig. 2D; grey area). A small but non-significant increase was observed in the AV-only group after 10 weeks. Reimplantation of the control CMV-GFP injected ventral roots results in a voluntary grip increase starting between 8 and 10 weeks post-reimplantation. Despite a gradual gain in grip strength, reimplantation of CMV-GFP treated roots only leads to a significant difference compared to AV-only group at the last time point (Fig. 2D, $p < 0.01$, grip strength 23.4 ± 2.2). In contrast, in dox-i-GDNF treated animals grip strength recovery was more progressive over time resulting in a final grip strength of 29.1 ± 3.8 at 20 weeks. Compared to AV-only, the grip strength in dox-i-GDNF treated animals was significantly improved starting from week 12 (Fig. 3D, p < 0.01). Already at 12 weeks, grip strength of the dox-i-GDNF treated animals reached the maximal grip strength obtained by the CMV-GFP group at 20 weeks. Despite a trend towards improved recovery ($p = 0.07$ at 14 weeks), no significant difference between CMV-GFP and dox-i-GDNF was observed. These observations show that there is a delay of approximately 2 weeks between the first electrophysiological CMAP response (Fig. 3C) and the occurrence of increased grip strength values. The data further show that cervical ventral root reimplantation alone resulted in increased CMAP amplitudes but had a poor effect on grip strength. Additional effects from dox-i-GDNF were not detected using electrophysiological testing, whereas an earlier and additive effect of dox-i-GDNF treatment on voluntary grip strength is demonstrated compared to AV-only.

3.3. Proximal application of timed GDNF treatment enhances motoneuron survival and axonal outgrowth

To determine the effects of timed GDNF expression on motoneuron survival, motoneurons were quantified in all animals 21 weeks post-surgery in ChAT stained spinal cord sections. Severe motoneuron atrophy and loss occurred in the ipsilateral motoneuron pool of AV-only animals compared to the many large ChAT-positive motoneurons present in the contralateral motoneuron pool (Fig. 4A-B). Quantification of the number of surviving motoneurons after AV-only reveals an average motoneuron survival of 38% (Fig. 4E). Implantation of control ventral roots injected with CMV-GFP leads to a significant increase in motoneuron survival of 66% on average (Fig. 4C, E, $p < 0.0001$). In addition to ventral root reimplantation, 4 week timed dox-i-GDNF treatment further increases motoneuron survival up to 81% (Fig. 4D, E, p < 0.0001 versus AV-only; $p < 0.005$ versus CMV-GFP). Although some smaller motoneuron profiles were observed (Fig. 4D arrowhead), dox-i-GDNF treated motoneurons appeared larger and healthier. Quantification of the motoneuron soma surface area reveals that following AV-only, surviving motoneurons have an average surface area of 51% compared to intact controls. Reimplantation of control CMV-GFP ventral roots leads to a partial rescue of the motoneuron size up to 83%. Reimplantation of dox-i-GDNF treated ventral roots results in a soma size of 118% compared to controls, indicating GDNF is inducing a small degree of hypertrophy. These results show that in addition to acute ventral root implantation, time-restricted dox-i-GDNF gene therapy significantly promotes motoneuron survival.

At 4 cm distal from the implantation site, an evaluation of the degree of axonal outgrowth towards the target musculature was performed in transverse median and ulnar peripheral nerve sections stained for ChAT. In intact nerves, large diameter ChAT positive axons are found as expected in patches distributed throughout the fascicle (Fig. 5A, B). In the AV-only group, despite avulsion of 4 ventral roots an average of 121 ± 42 small diameter regenerating motor axons were quantified (Fig. 5C, arrowheads). No large diameter axons were present in these animals, confirming lesion completeness and suggesting these are regenerating fibers. In the CMV-GFP control group, reimplantation

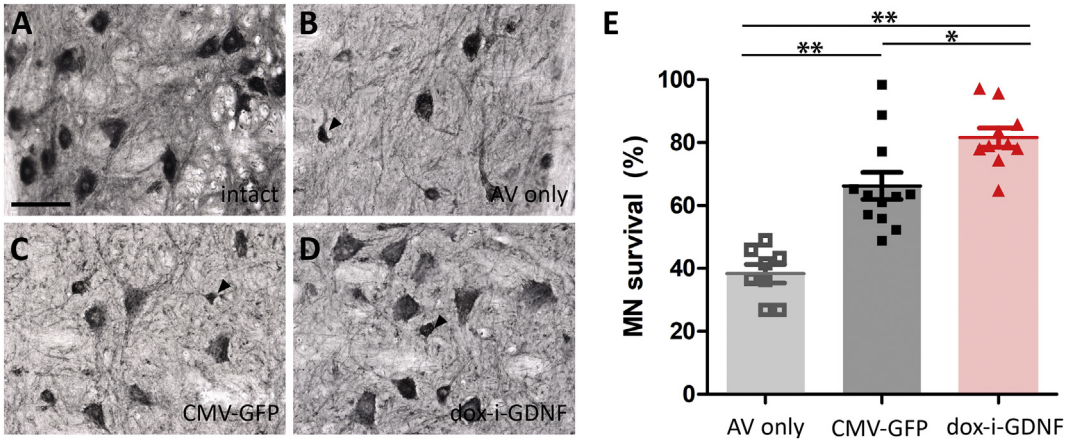

Fig. 4. Timed GDNF gene therapy promotes motoneuron survival. (A–D) Representative images of the spinal motoneuron pool stained for ChAT. Compared to intact contralateral motoneurons (A), AV-only leads to severe motoneuron loss and motoneuron atrophy (B; arrowhead). (C) Reimplantation of control CMV-GFP transduced ventral roots reduced motoneuron death but many atrophic motoneurons are observed (arrowhead). (D) Timed dox-i-GDNF treatment appeared to normalize the cellular morphology and further increases motoneuron survival. (E) Quantification of the number of $ChAT^{+}$ neurons reveals additional motoneuron survival in dox-i-GDNF treated animals compared to implantation of CMV-GFP control ventral roots. * $p < 0.005$, ** $p < 0.0001$. Arrowheads in B–D point to atrophic motoneurons. Scale bar in A (A–D) 75 µm. Data represent individual animals and expressed as mean ± SEM.

of avulsed roots facilitated axonal outgrowth and regeneration of axons towards the peripheral nerve. The ulnar and median nerves from these animals contained 275 ± 48 axons, which were homogeneously distributed throughout the nerve (Fig. 5D, $p < .02$ versus AV-only). Four week GDNF expression results in a further increase in the number of small diameter regenerating axons. Quantification reveals a significant 1.7 fold increase in the number of axons (487 ± 66) compared to CMV-GFP animals (Fig. 5E, F; $p < .0003$ versus AV-only; $p < 0.008$ versus CMV-GFP). Combined, these data show that timed GDNF treatment improves motoneuron survival as well as distal axonal regeneration.

The number of motoneurons that were able to reach the palmar musculature 6.5 cm distal to the lesion and repair site, was assessed in every fourth spinal cord section by quantification of the number of

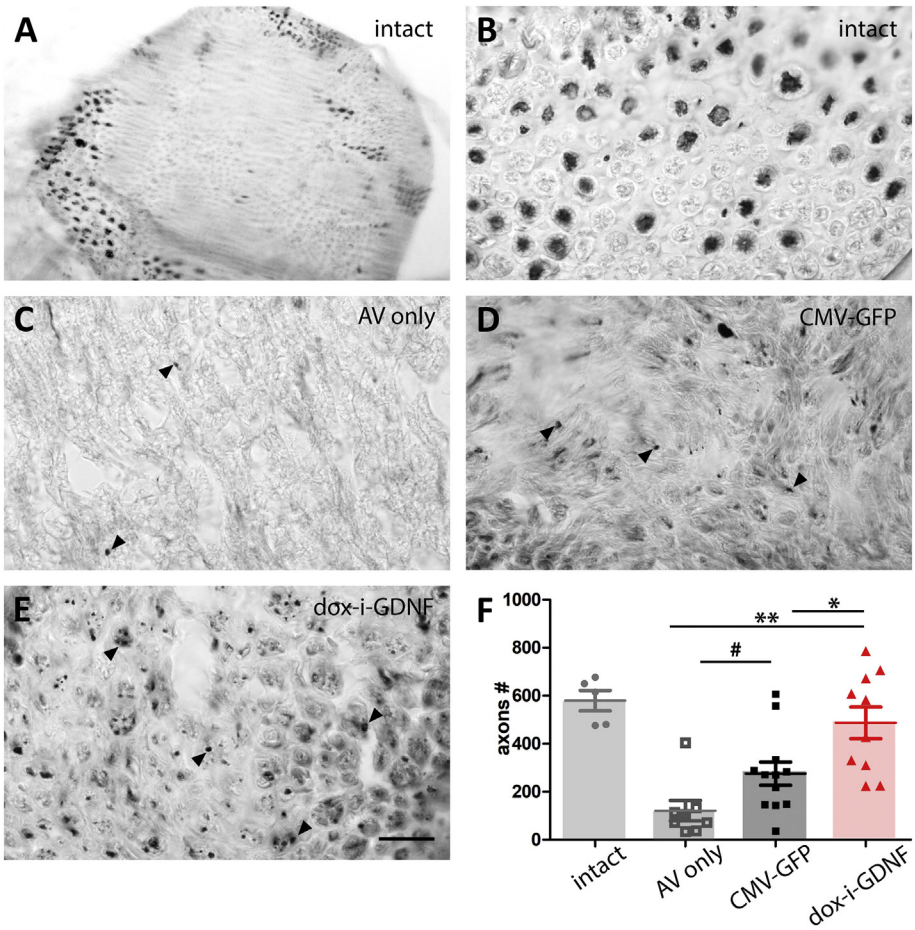

Fig. 5. Timed GDNF expression in the ventral root improves axonal outgrowth into median and ulnar nerves. (A–F) Representative ChAT stained images of transverse median and ulnar nerve sections 4 cm distal from the implantation site 21 weeks post lesion. (A, B) A low and high magnification of an intact nerve shows expected heterogeneous distribution of large diameter intact motor axons. (C) After AV-only, few and small axons are found in the peripheral nerves. (D) Reimplantation of ventral roots facilitates axonal outgrowth and regeneration into the peripheral nerves, resulting in increased axon counts. (E) In dox-i-GDNF animals, timed 4 week GDNF expression leads to a further increase in the number of regenerating axons at 4 cm distal. (F) Quantification of the number of motor axons in both median and ulnar nerves reveals a 1,7 fold increase following dox-i-GDNF treatment. ** $p < 0.0003$, * $p < 0.008$, # $p < 0.02$. Arrowheads in C–E indicate ChAT positive regenerating axons. Scale bar in E (B–E) 15 µm. Data represent individual animals and expressed as mean ± SEM.

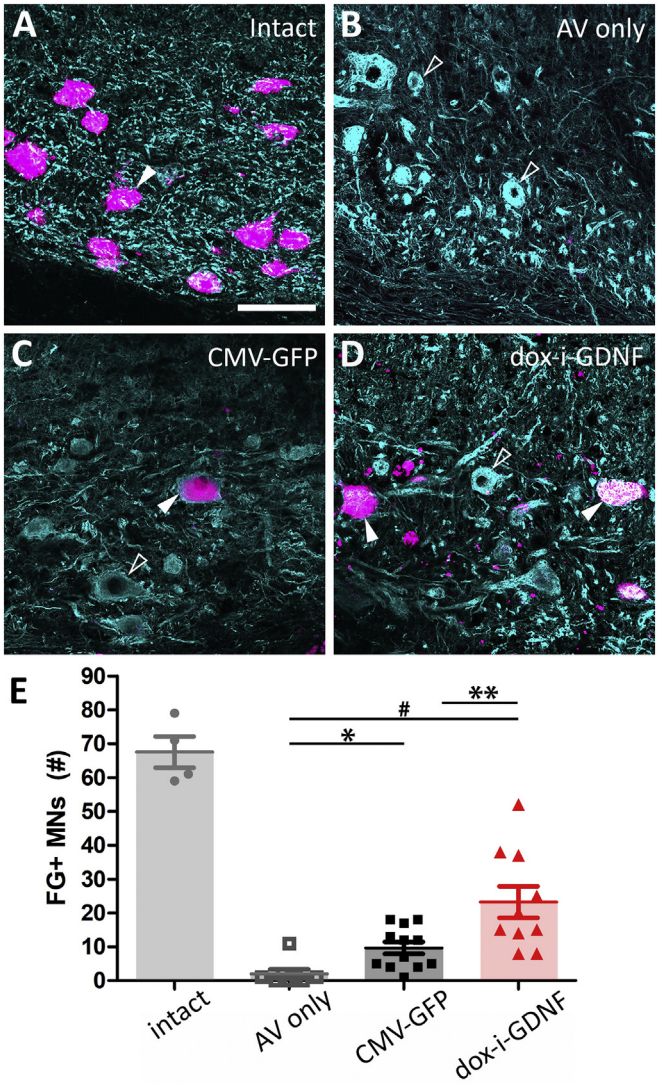

Fig. 6. Timed GDNF gene therapy improves distal axon outgrowth. (A–D) Representative images of motoneurons retrogradely traced from the intrinsic hand musculature located approximately 6,5 cm distal from the implantation site (tubulin-β3; cyan, Fluoro Gold (FG); magenta). (A) A cluster of motoneurons innervating the hand musculature in intact animals in the ventral motoneuron pool. (B) After AV-only, tubulin-β3 staining reveals atrophic motoneurons (open arrowhead) whereas FG^+ motoneurons are absent. (C) Reimplantation in CMV-GFP animals leads to a small increase in FG^+ motoneurons. (D) dox-i-GDNF treatment significantly increased the number of FG^+ positive motoneurons. (E) Quantification reveals dox-i-GDNF treatment more than doubled the number of FG^+ motoneurons, indicating improved distal regeneration after timed GDNF expression. # $p < 0.0006$, ** $p < 0.0042$. * $p < 0.0026$. Solid white arrowheads in A–D point to retrogradely traced motoneuron, open arrowheads indicate surviving non-traced motoneuron. Scale bar in A (A-D) 100 µm. Data represent individual animals and expressed as mean ± SEM. (For interpretation of the references to colour in this figure legend, the reader is referred to the web version of this article.)

retrogradely traced FG^+ neurons. In non-lesioned animals, an average of 67.5 ± 4.3 retrogradely traced FG^+ motoneurons was present. In the AV-only group retrogradely traced motoneurons were rarely observed (2.0 ± 1.3 motoneurons; Fig. 6B). Reimplantation of CMV-GFP injected ventral roots results in an average of 9.6 ± 1.7 motoneurons that regenerated an axon towards the denervated palm musculature. In contrast, dox-i-GDNF treatment more than doubles the number of retrogradely traced motoneurons (23.1 ± 4.6) compared to CMV-GFP (Fig. 6D, $p < 0.004$). Taken together, 4 week time-restricted dox-i-GDNF gene therapy significantly promoted motoneuron survival and enhanced axon regeneration in the peripheral nerve and towards the distal palmar musculature.

3.4. Distal musculature innervation

To investigate whether timed GDNF treatment leads to enhanced distal target muscle reinnervation, quantification of the number of reinnervated endplates was performed in the intrinsic paw musculature which encompasses the thenar, hypothenar and lumbrical muscles. In sections stained for presynaptic nerve terminals and postsynaptic AChR clusters, overlap between nerve terminals and the AChR cluster was scored. In control muscle, innervating motor and sensory axons (Fig. 7A, green) are found following the motor endplate bands (red). The typical complete overlap of the nerve terminal and postsynaptic AChR clusters can be appreciated at high magnification (Fig. 7B-D). At 21 weeks after AV-only, most AChR clusters had a normal morphology, but a significant loss of innervated endplates was observed. Despite the fact that the ventral roots were not reimplanted, tubulin-β3 positive afferent and efferent axons are present and in 35 ± 8.3% of the endplates some degree of presynaptic nerve terminal overlap was observed. In the majority of end plates, this overlap appeared to be only partial (Fig. 7H, open arrowhead). An increase in innervated endplates up to 80.2 ± 3.8% occurs after ventral root reimplantation in CMV-GFP treated animals (Fig. 7I, $p < 0.0001$ versus AV-only). In addition to reimplantation, dox-i-GDNF treatment further increases endplate innervation up to 92.1 ± 3.7% ($p < 0.005$ versus CMV-GFP). Here, the staining of AChR clusters and nerve terminals almost fully overlapped in the majority of endplates (Fig. 7P, closed arrowhead). Together with the twofold increased number of retrogradely traced motoneurons from this muscle in the dox-i-GDNF group, this indicates that the increased NMJ innervation is not due to local sprouting and motor unit enlargement alone, but timed GDNF treatment leads to improved muscle reinnervation.

3.5. Associations between histological and functional parameters

Regression analysis on end-point function test data and histological quantifications of individual animals was performed to examine the existence of predictive relationships. In all scatter plots examined, a clear hierarchy was observed with a cluster of AV-only animals present in the bottom left and the majority of the dox-i-GDNF treated animals in the top-right cluster (Fig. 8). The two strongest predictive values are found between the degree of motoneuron survival and number of regenerating distal axons ($p < .0001$; $R^2 = 0,30$) and the percentage of innervated neuromuscular junctions and CMAP amplitude ($p < 0.0001$; $R^2 = 0,58$). Comparable coefficients exist between the recovery of grip strength and number of innervated endplates or motoneuron survival ($p < 0.001$; $R^2 = 0,32$, $p < 0.0017$; $R^2 = 0,30$ respectively). The associations found between improved histological outcomes and the degree of recovery of function emphasize the additive beneficial effect of dox-i-GDNF.

4. Discussion

Lumbar and cervical plexus lesions are severe proximal nerve lesions. We have recently shown that timed GDNF gene therapy in a lumbar plexus injury model promotes axon regeneration and improves electrophysiological recovery but failed to stimulate voluntary hind paw function (Eggers et al., 2019). In the current study we examined whether timed GDNF gene therapy can enhance regeneration and functional recovery following cervical ventral root reimplantation. Following a cervical avulsion, regenerating axons have to bridge only half the distance (6,5 cm) they have to grow after a lumber lesion (10 to 13 cm) before reaching the most distal muscles. We show that dox-i-GDNF treatment promotes the survival of cervical motor neurons and

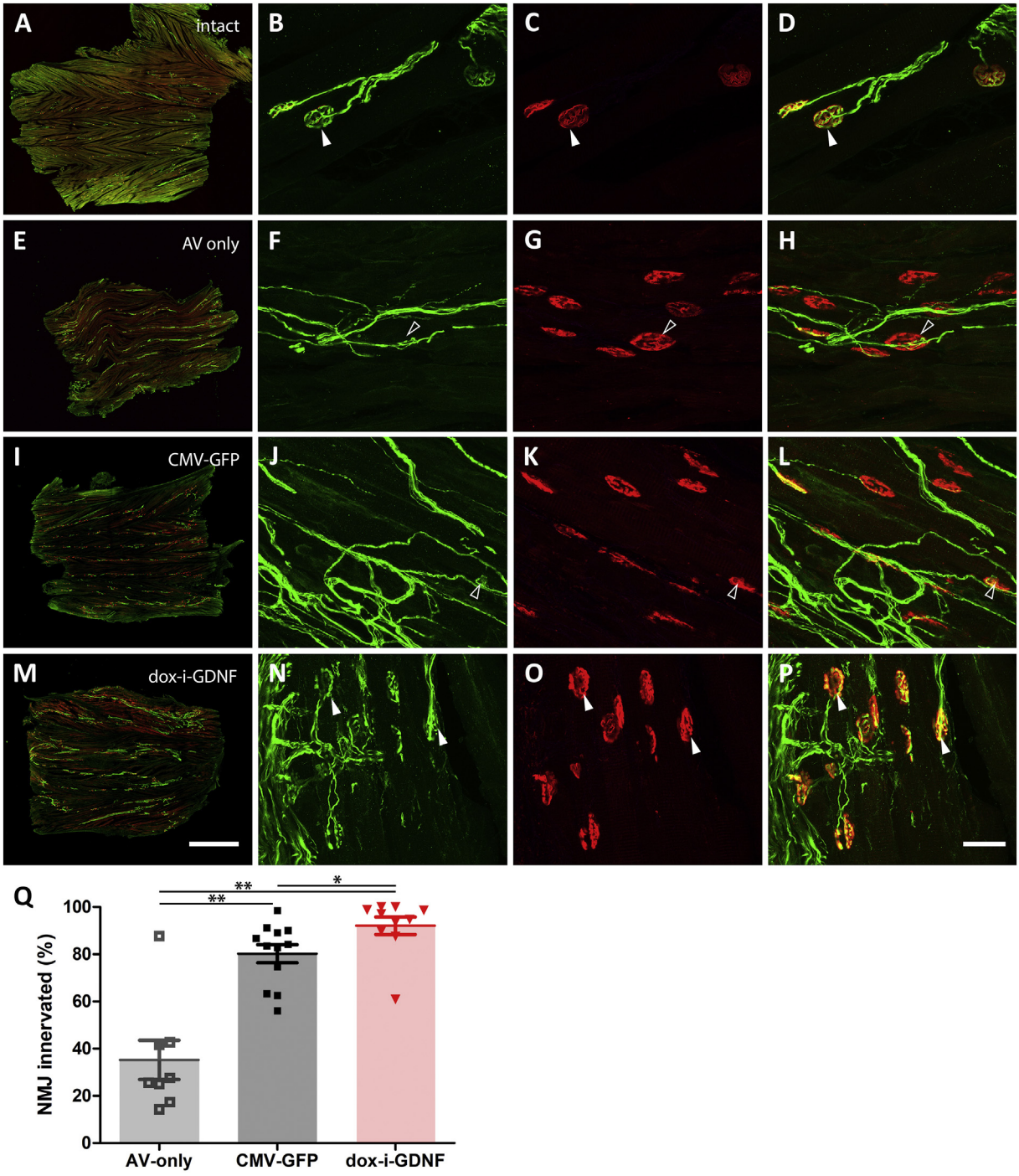

Fig. 7. Timed GDNF gene therapy promotes distal target muscle reinnervation. (A–Q) Representative images of palmar musculature 21 weeks post surgery. Intact (A–D), avulsion-only (E–H), CMV-GFP (I–L) and dox-i-GDNF (M–P) animals stained for presynaptic nerve terminals and postsynaptic AChR clusters (tubulin-β3 and SV-2; green, BTX; red). (A) Low magnification in intact animals showing innervating motor and sensory axons following the motor endplate bands. (B–D) Complete intact innervation shown by the overlap of the nerve terminal and postsynaptic AChR clusters at high magnification. (E) After AV-only, at low magnification muscle atrophy is evident. (F–H) AChR clusters 21 weeks after AV-only show the majority of innervated endplates had a partial nerve terminal overlap**.** (J–L) Increased endplate innervation was observed in CMV-GFP treated animals (arrowhead**).** (N–P) Timed dox-i-GDNF treatment further increases endplate innervation, with the majority of the AChR clusters and nerve terminals almost fully overlapped. (Q) Quantification of the number of endplates that were partially or completely innervated. * $p < 0.005$, ** $p < 0.0001$. Arrowheads in A-D point to innervated endplates, open arrowheads indicate partial innervation. Scale bar in M (A, E, I, M): 1000 μm, P (B–D, F–H, J–L, N–P) 25 μm. (For interpretation of the references to colour in this figure legend, the reader is referred to the web version of this article.)

axon regeneration as was previously observed after a lumbar plexus lesion. Importantly, following a cervical lesion dox-i-GDNF stimulated recovery of forepaw grip strength. These functional improvements were associated with an increase in the reinnervation of the muscles in the denervated hand musculature. This study marks an important step in demonstrating that dox-i-GDNF treatment can exert functional benefit after a severe proximal nerve lesion relatively close to the target organ.

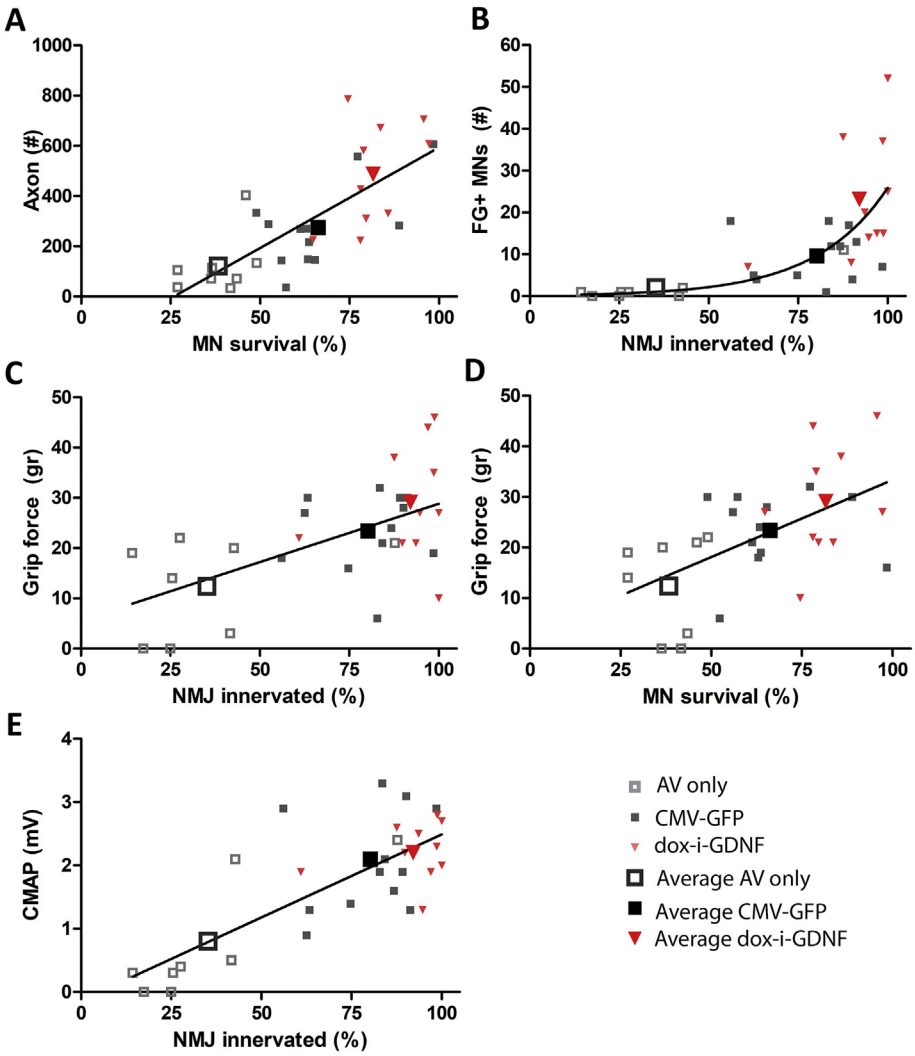

Fig. 8. Regression analysis discloses predictive relationships between functional and histological output parameters. (A–E) Scatter plots of end-point data including motoneuron survival, distal axonal growth, NMJ innervation, CMAP response or grip strength. Simple regression calculation was performed to examine predictive relationships. (A) Significant regression equations were found between the degree of motoneuron survival and distal axon number. Regression coefficients indicate predictive relationships between the degree of endplate innervation and (B) retrogradely traced motoneurons and (C) generated grip force. (D) Increasing motoneuron survival has a predictive value for increased grip force. (E) The percentage of innervated endplates is associated with enhanced CMAP amplitudes. (A; $F_{(1.28)} = 34{,}56$, $p < 0.0001$ with an R^2 of 0,30. B; $F_{(1.28)} = 16{,}56$, $p < 0.0003$ with an R^2 of 0,372. C; $F_{(1.28)} = 13.53$, $p < .001$ with an R^2 of 0,32. D; $F_{(1.28)} = 12.05$, $p < 0.0017$ with an R^2 of 0,30. E; $F_{(1.28)} = 34.56$, $p < 0.0001$ with an R^2 of 0,58). Data represent individual animals. One large symbol per group indicates group averages.

4.1. Timed GDNF treatment enhances motoneuron survival, axon regeneration and muscle reinnervation

Regeneration following a severe ventral root lesion is poor due to the gradual degeneration of motoneurons and because Schwann cells remain supportive of axon regeneration for only a limited time window. We show that four week timed dox-i-GDNF treatment of an elaborate cervical ventral root lesion promotes motoneuron survival up to 21 weeks post-lesion. Long lasting neuroprotective effects of time-restricted GDNF gene therapy is in agreement with previous observations in a lumber plexus lesion (Eggers et al., 2019). GDNF is a potent motoneuron survival factor (Henderson et al., 1994) and application of GDNF protein after cervical root avulsion consistently improved motoneuron survival (Li et al., 1995; Watabe et al., 2000; Yuan et al., 2000; Wu et al., 2003; Zhou and Wu, 2006). Delivery of GDNF, however, needs to be performed as early as possible after avulsion, as delayed application at 2 weeks, but not at 4 weeks post-lesion results in improved motoneuron survival (Zhou and Wu, 2006).

We demonstrate here that timed dox-i-GDNF treatment also significantly enhanced distal axon regeneration and reinnervation of the intrinsic hand muscles. This extends and corroborates earlier proof of concept studies in the distal peripheral nerve where controlled GDNF delivery results in improved axonal regeneration (Shakhbazau et al., 2013; Marquardt et al., 2015; Tajdaran et al., 2016). Application of GDNF protein after cervical ventral root reimplantation using either topical application or direct nerve injection, promoted axonal outgrowth up to 2 cm (Chu and Wu, 2009; Chu et al., 2012). Importantly, more regenerating axons enter the reimplanted nerve graft when GDNF was applied inside the nerve, but no functional improvement was reported. Application of gelfoam soaked GDNF at the spinal cord surface however, did not result in improved recovery of function following a 2 week delayed C6 root reimplantation (Ruven et al., 2018). These observations suggest that GDNF should be delivered inside the nerve in order to exert a beneficial effect. GDNF gene delivery to the reimplanted nerve root as employed in this study, ensures continued secretion of GDNF in the denervated nerve where it attracts axons and promotes axon extension.

4.2. Timed GDNF treatment promotes functional recovery when the lesion is applied within a critical distance of the target muscle

The absence of voluntary functional recovery following dox-i-GDNF treatment in a lumbar plexus injury may be due to the deterioration of the Schwann cells in the distal nerve occurring as a result of prolonged nerve denervation (Giannini and Dyck, 1990; Funakoshi et al., 1993; Fu and Gordon, 1995; Sulaiman and Gordon, 2000; Hoke et al., 2002; Gordon et al., 2011). After a critical period of 6 to 8 weeks post lesion, denervated Schwann cells gradually fail to support axon regeneration and a state of chronic denervation develops. Following lumbar plexus avulsion the initial velocity of axon regeneration into the proximal nerve is 1 to 2 mm/day, however, the growth speed of the fastest growing axons declines to < 1 mm/day (Eggers et al., 2010). Here, we

examined dox-i-GDNF treatment after a cervical ventral root reimplantation, which in comparison to lumbar ventral root reimplantation requires a shorter regeneration distance towards the target muscle. The majority of root avulsion studies are performed using cervical ventral roots. Most frequently, an avulsion of 1 or 3 ventral roots is applied after which axonal regeneration is assessed close to the reimplantation site (Haninec et al., 2004; Pinter et al., 2010; Chu et al., 2012; Li et al., 2015; Fang et al., 2016; Gloviczki et al., 2017; Ruven et al., 2018; Wang et al., 2019). To achieve our aim of reliably monitoring the recovery of hand function and to prevent sprouting from intact adjacent nerves, complete denervation of the distal flexor muscles by avulsion of C6, C7, C8 and T1 ventral roots was mandatory (Bertelli et al., 1995; McKenna et al., 2000; Tosolini and Morris, 2012). We show for the first time that timed GDNF gene therapy enhanced recovery of voluntary grip strength after cervical ventral root reimplantation. Importantly, we show significant associations between the degree of functional recovery and our histological outcomes. This demonstrates the additive beneficial effect of timed GDNF treatment. Here, the first electrophysiological signs of distal muscle reinnervation occur at 6 weeks and this is closely followed by increased grip strength. All reimplanted animals displayed a CMAP response at 12 weeks. This timing suggests axons were able to regenerate during the critical first 8 weeks through a pro-regenerative or sub-chronic peripheral nerve before reaching the hand musculature. Combined, these results demonstrate the robust effects of proximal timed GDNF-gene therapy following spinal nerve avulsion lesions. Our observed muscle reinnervation at 6,5 cm distance occurs just within the critical 8 week period, suggesting that beyond this distance regeneration becomes increasingly poor.

In agreement with studies performing cervical ventral root reimplantation without additional intervention, we find a moderate degree of axonal regeneration and recovery of the denervated forepaw in untreated rats (Gu et al., 2004; Huang et al., 2009; Pinter et al., 2010; Li et al., 2015; Fang et al., 2016; Gloviczki et al., 2017; Ruven et al., 2018). This observed spontaneous regeneration after reimplantation of CMV-GFP treated roots, could explain the absence of an increased CMAP response after timed GDNF treatment. Following chronic and partial denervation, a decline in regenerative capacity can be fully compensated by enlargement of motor units, which have been estimated to reach up to 3 to 5 times their original size (Brown and Ironton, 1978; Fu and Gordon, 1995; Gordon et al., 2011). However, when maximal motorunit enlargement occurs but $< 25\%$ of the motoneurons remain, this prevents full recovery of the muscle contractile force (Rafuse et al., 1992; Gordon and Tyreman, 2010; Gordon et al., 2011). We find that although following CMV-GFP root reimplantation only 14% of the motoneurons regenerated an axon into the distal musculature, they reinnervated 80% of the endplates. In contrast, regeneration of 34% of motoneurons into the distal musculature after dox-i-GDNF treatment leads to a modest improvement towards 92% of endplate reinnervation. These underlying mechanisms could account for the observed comparable high degree of endplate reinnervation, at which point small differences between groups are no longer detected using CMAP measurements. The enhanced number of motoneurons innervating the distal musculature after dox-i-GDNF treatment however, does increase the recovery of contractile force as observed in our grip strength.

Although reinnervation of flexor muscle groups resulted in enhanced recovery of grip strength, fine motor skills requires an interplay between flexor and extensor muscles. Skilled fine motor movement of the wrist and fingers was however not studied. Reinnervation of the appropriate muscle is of importance as axonal misdirection could lead to co-contractions of the antagonistic musculature (Hallin et al., 1999). To determine the degree of correct reinnervation, further analysis using function tests such as forepaw kinematic motion analysis (Wang et al., 2008; Burnside et al., 2018), and retrograde tracing from specific muscle groups (Tosolini and Morris, 2012) could be beneficial.

4.3. Future perspectives

The three key factors limiting recovery of function after ventral root avulsion injury are progressive motoneuron degeneration, poor long distance regeneration and the deleterious effect of chronic denervation on the condition of the muscle. This study underscores the exceptional potency of proximal timed GDNF-gene therapy as reflected in enhanced functional recovery due to sustained motoneuron survival and enhanced axonal regeneration. Proximal GDNF treatment, however, does not counteract the inhibitory environment of the denervated distal nerve and has no impact on the chronically denervated muscle. To address these issues additional treatments are required.

Examples of such treatments include electrical, pharmacological, molecular and novel surgical interventions. Specifically treatments such as brief electrical stimulation or FDA approved pharmacological compound treatments are of great significance due to their potential direct clinical applicability. Brief electrical stimulation of injured nerves promoted axon regeneration and has recently shown promise in human patients (Wong et al., 2015; Senger et al., 2019). Systemic 'neuroheal' treatment, consisting of two existing pharmacological compounds selected based upon their ability to target predefined molecules or pathways, exerted beneficial effects on motoneuron survival, axon outgrowth and muscle atrophy (Romeo-Guitart et al., 2017; Romeo-Guitart et al., 2018). Recent molecular strategies aimed at counteracting inhibitory signaling at the implantation site and inside denervated nerves are emerging as valuable treatments to promote long distance regeneration (Sabatier et al., 2012; Joshi et al., 2015; Li et al., 2015; Guo et al., 2019). Finally, to prevent the negative impact of chronic muscle denervation (Bain et al., 2001; Ma et al., 2011; Sakuma et al., 2016) surgical rerouting of a local intact motor or sensory nerve can be used to temporarily innervate the denervated distal nerve and its denervated muscle targets (Bain et al., 2001; Sulaiman and Gordon, 2018). This "baby-sitting" technique protected the Schwann cells and muscle from the deleterious effect of chronic denervation resulting in reduced muscle atrophy while long distance regeneration is in progress. By combining these strategies in future research, the resulting multilevel intervention would provide improved motoneuron survival while at the same time keeping the distal nerve and musculature in a state that is permissive for long-distance axon regeneration and muscle reinnervation.

Author contributions

RE, FdW, MRT and JV conceived and designed the study. RE, CA and FdW conducted experiments and analysed the data. FdW provided essential reagents. RE and JV wrote the manuscript, with input from the other authors.

Declaration of Competing Interest

The authors report no competing interests.

Acknowledgements

This work was supported by grants from the Wings for Life Spinal Cord Research Foundation (WFL-NL17/16 to J.V) and International Spinal Research Trust (TRI004_03 to J.V.).

References

Abe, N., Cavalli, V., 2008. Nerve injury signaling. Curr. Opin. Neurobiol. 18, 276–283.
Arthur-Farraj, P.J., Latouche, M., Wilton, D.K., Quintes, S., Chabrol, E., Banerjee, A., Woodhoo, A., Jenkins, B., Rahman, M., Turmaine, M., Wicher, G.K., Mitter, R., Greensmith, L., Behrens, A., Raivich, G., Mirsky, R., Jessen, K.R., 2012. c-Jun reprograms Schwann cells of injured nerves to generate a repair cell essential for regeneration. Neuron 75, 633–647.
Arthur-Farraj, P.J., Morgan, C.C., Adamowicz, M., Gomez-Sanchez, J.A., Fazal, S.V.,

Beucher, A., Razzaghi, B., Mirsky, R., Jessen, K.R., Aitman, T.J., 2017. Changes in the coding and non-coding Transcriptome and DNA Methylome that define the Schwann cell repair phenotype after nerve injury. Cell Rep. 20, 2719–2734.
Bain, J.R., Veltri, K.L., Chamberlain, D., Fahnestock, M., 2001. Improved functional recovery of denervated skeletal muscle after temporary sensory nerve innervation. Neuroscience 103, 503–510.
Bergerot, A., Shortland, P.J., Anand, P., Hunt, S.P., Carlstedt, T., 2004. Co-treatment with riluzole and GDNF is necessary for functional recovery after ventral root avulsion injury. Exp. Neurol. 187, 359–366.
Bertelli, J.A., Taleb, M., Saadi, A., Mira, J.C., Pecot-Dechavassine, M., 1995. The rat brachial plexus and its terminal branches: an experimental model for the study of peripheral nerve regeneration. Microsurgery 16, 77–85.
Brown, M.C., Ironton, R., 1978. Sprouting and regression of neuromuscular synapses in partially denervated mammalian muscles. J. Physiol. 278, 325–348.
Brushart, T.M., Aspalter, M., Griffin, J.W., Redett, R., Hameed, H., Zhou, C., Wright, M., Vyas, A., Hoke, A., 2013. Schwann cell phenotype is regulated by axon modality and central-peripheral location, and persists in vitro. Exp. Neurol. 247, 272–281.
Burnside, E.R., De Winter, F., Didangelos, A., James, N.D., Andreica, E.C., Layard-Horsfall, H., Muir, E.M., Verhaagen, J., Bradbury, E.J., 2018. Immune-evasive gene switch enables regulated delivery of chondroitinase after spinal cord injury. Brain. 141 (8), 2362–2381. https://doi.org/10.1093/brain/awy158. August.
Chai, H., Wu, W., So, K.F., Prevette, D.M., Oppenheim, R.W., 1999. Long-term effects of a single dose of brain-derived neurotrophic factor on motoneuron survival following spinal root avulsion in the adult rat. Neurosci.Lett. 274, 147–150.
Chu, T.H., Wu, W., 2009. Neurotrophic factor treatment after spinal root avulsion injury. Cent. Nerv. Syst. Agents Med. Chem. 9, 40–55.
Chu, T.H., Wang, L., Guo, A., Chan, V.W., Wong, C.W., Wu, W., 2012. GDNF-treated acellular nerve graft promotes motoneuron axon regeneration after implantation into cervical root avulsed spinal cord. Neuropathol. Appl. Neurobiol. 38, 681–695.
Eggers, R., Hendriks, W.T., Tannemaat, M.R., van Heerikhuize, J.J., Pool, C.W., Carlstedt, T.P., Zaldumbide, A., Hoeben, R.C., Boer, G.J., Verhaagen, J., 2008. Neuroregenerative effects of lentiviral vector-mediated GDNF expression in re-implanted ventral roots. Mol.Cell Neurosci. 39, 105–117.
Eggers, R., Tannemaat, M.R., Ehlert, E.M., Verhaagen, J., 2010. A spatio-temporal analysis of motoneuron survival, axonal regeneration and neurotrophic factor expression after lumbar ventral root avulsion and implantation. Exp.Neurol. 223, 207–220.
Eggers, R., de Winter, F., Hoyng, S.A., Hoeben, R.C., Malessy, M.J.A., Tannemaat, M.R., Verhaagen, J., 2019. Timed GDNF gene therapy using an immune-evasive gene switch promotes long distance axon regeneration. Brain 142, 295–311.
Fang, X.Y., Zhang, W.M., Zhang, C.F., Wong, W.M., Li, W., Wu, W., Lin, J.H., 2016. Lithium accelerates functional motor recovery by improving remyelination of regenerating axons following ventral root avulsion and reimplantation. Neuroscience 329, 213–225.
Fu, S.Y., Gordon, T., 1995. Contributing factors to poor functional recovery after delayed nerve repair: prolonged denervation. J.Neurosci. 15, 3886–3895.
Funakoshi, H., Frisen, J., Barbany, G., Timmusk, T., Zachrisson, O., Verge, V.M., Persson, H., 1993. Differential expression of mRNAs for neurotrophins and their receptors after axotomy of the sciatic nerve. J. Cell Biol. 123, 455–465.
Giannini, C., Dyck, P.J., 1990. The fate of Schwann cell basement membranes in permanently transected nerves. J.Neuropathol.Exp.Neurol. 49, 550–563.
Gloviczki, B., Torok, D.G., Marton, G., Gal, L., Bodzay, T., Pinter, S., Nogradi, A., 2017. Delayed spinal cord-brachial plexus reconnection after C7 ventral root avulsion: the effect of reinnervating motoneurons rescued by Riluzole treatment. J. Neurotrauma 34, 2364–2374.
Gordon, T., Tetzlaff, W., 2015. Regeneration-associated genes decline in chronically injured rat sciatic motoneurons. Eur. J. Neurosci. 42, 2783–2791.
Gordon, T., Tyreman, N., 2010. Sprouting capacity of lumbar motoneurons in normal and hemisected spinal cords of the rat. J. Physiol. 588, 2745–2768.
Gordon, T., Tyreman, N., Raji, M.A., 2011. The basis for diminished functional recovery after delayed peripheral nerve repair. J. Neurosci. 31, 5325–5334.
Gu, H.Y., Chai, H., Zhang, J.Y., Yao, Z.B., Zhou, L.H., Wong, W.M., Bruce, I., Wu, W.T., 2004. Survival, regeneration and functional recovery of motoneurons in adult rats by reimplantation of ventral root following spinal root avulsion. Eur.J.Neurosci. 19, 2123–2131.
Guo, W.L., Qi, Z.P., Yu, L., Sun, T.W., Qu, W.R., Liu, Q.Q., Zhu, Z., Li, R., 2019. Melatonin combined with chondroitin sulfate ABC promotes nerve regeneration after root-avulsion brachial plexus injury. Neural Regen. Res. 14, 328–338.
Hallin, R.G., Carlstedt, T., Nilsson-Remahl, I., Risling, M., 1999. Spinal cord implantation of avulsed ventral roots in primates; correlation between restored motor function and morphology. Exp. Brain Res. 124, 304–310.
Haninec, P., Dubovy, P., Samal, F., Houstava, L., Stejskal, L., 2004. Reinnervation of the rat musculocutaneous nerve stump after its direct reconnection with the C5 spinal cord segment by the nerve graft following avulsion of the ventral spinal roots: a comparison of intrathecal administration of brain-derived neurotrophic factor and Cerebrolysin. Exp. Brain Res. 159, 425–432.
Henderson, C.E., Phillips, H.S., Pollock, R.A., Davies, A.M., Lemeulle, C., Armanini, M., Simpson, L.C., Moffet, B., Vandlen, R.A., Koliatsos, V.E., Arnon, R., 1994. GDNF: a potent survival factor for Mmotoneurons present in peripheral nerve and muscle. Science 266, 1062–1064.
Hendriks, W.T., Eggers, R., Carlstedt, T.P., Zaldumbide, A., Tannemaat, M.R., Fallaux, F.J., Hoeben, R.C., Boer, G.J., Verhaagen, J., 2007. Lentiviral vector-mediated reporter gene expression in avulsed spinal ventral root is short-term, but is prolonged using an immune "stealth" transgene. Restor. Neurol. Neurosci. 25, 585–599.
Hoke, A., Gordon, T., Zochodne, D.W., Sulaiman, O.A., 2002. A decline in glial cell-line-derived neurotrophic factor expression is associated with impaired regeneration after long-term Schwann cell denervation. Exp. Neurol. 173, 77–85.
Huang, M.C., Lo, M.J., Lin, Y.L., Chang, S.E., Huang, W.C., Kuo, W.C., Tsai, M.J., Kuo, H.S., Shih, Y.H., Cheng, H., 2009. Functional recovery after the repair of transected cervical roots in the chronic stage of injury. J. Neurotrauma 26, 1795–1804.
Jessen, K.R., Mirsky, R., 2002. Signals that determine Schwann cell identity. J. Anat. 200, 367–376.
Jessen, K.R., Mirsky, R., 2016. The repair Schwann cell and its function in regenerating nerves. J. Physiol. 594, 3521–3531.
Joshi, A.R., Bobylev, I., Zhang, G., Sheikh, K.A., Lehmann, H.C., 2015. Inhibition of Rho-kinase differentially affects axon regeneration of peripheral motor and sensory nerves. Exp. Neurol. 263, 28–38.
Kachramanoglou, C., Carlstedt, T., Koltzenburg, M., Choi, D., 2017. Long-term outcome of brachial plexus reimplantation after complete brachial plexus avulsion injury. World Neurosurg. 103, 28–36.
Koliatsos, V.E., Price, W.L., Pardo, C.A., Price, D.L., 1994. Ventral root avulsion: an experimental model of death of adult motor neurons. J. Comp. Eurol. 342, 35–44.
Li, L., Wu, W., Lin, L.F., Lei, M., Oppenheim, R.W., Houenou, L.J., 1995. Rescue of adult mouse motoneurons from injury-induced cell death by glial cell line-derived neurotrophic factor. Proc. Natl. Acad. Sci. 92, 9771–9775.
Li, H., Wong, C., Li, W., Ruven, C., He, L., Wu, X., Lang, B.T., Silver, J., Wu, W., 2015. Enhanced regeneration and functional recovery after spinal root avulsion by manipulation of the proteoglycan receptor PTPsigma. Sci. Rep. 5, 14923.
Ma, C.H., Omura, T., Cobos, E.J., Latremoliere, A., Ghasemlou, N., Brenner, G.J., van Veen, E., Barrett, L., Sawada, T., Gao, F., Coppola, G., Gertler, F., Costigan, M., Geschwind, D., Woolf, C.J., 2011. Accelerating axonal growth promotes motor recovery after peripheral nerve injury in mice. J. Clin. Invest. 121, 4332–4347.
Marquardt, L.M., Ee, X., Iyer, N., Hunter, D., Mackinnon, S.E., Wood, M.D., Sakiyama-Elbert, S.E., 2015. Finely tuned temporal and spatial delivery of GDNF promotes enhanced nerve regeneration in a long nerve defect model. Tissue Eng. Part A 21, 2852–2864.
Mason, M.R., Lieberman, A.R., Anderson, P.N., 2003. Corticospinal neurons up-regulate a range of growth-associated genes following intracortical, but not spinal, axotomy. Eur. J. Neurosci. 18, 789–802.
McKenna, J.E., Prusky, G.T., Whishaw, I.Q., 2000. Cervical motoneuron topography reflects the proximodistal organization of muscles and movements of the rat forelimb: a retrograde carbocyanine dye analysis. J. Comp. Neurol. 419, 286–296.
Naldini, L., Blomer, U., Gallay, P., Ory, D., Mulligan, R., Gage, F.H., Verma, I.M., Trono, D., 1996. In vivo gene delivery and stable transduction of nondividing cells by a lentiviral vector. Science 272, 263–267.
Penas, C., Casas, C., Robert, I., Fores, J., Navarro, X., 2009. Cytoskeletal and activity-related changes in spinal motoneurons after root avulsion. J. Neurotrauma 26, 763–779.
Piehl, F., Hammarberg, H., Hokfelt, T., Cullheim, S., 1998. Regulatory effects of trophic factors on expression and distribution of CGRP and GAP-43 in rat motoneurons. J. Neurosci. Res. 51, 1–14.
Pinter, S., Gloviczki, B., Szabo, A., Marton, G., Nogradi, A., 2010. Increased survival and reinnervation of cervical motoneurons by riluzole after avulsion of the C7 ventral root. J. Neurotrauma 27, 2273–2282.
Rafuse, V.F., Gordon, T., Orozco, R., 1992. Proportional enlargement of motor units after partial denervation of cat triceps surae muscles. J. Neurophysiol. 68, 1261–1276.
Risling, M., Ochsman, T., Carlstedt, T., Linda, H., Plantman, S., Rostami, E., Angeria, M., Skold, M.K., 2011. On acute gene expression changes after ventral root replantation. Front. Neurol. 1, 159.
Romeo-Guitart, D., Fores, J., Navarro, X., Casas, C., 2017. Boosted regeneration and reduced denervated muscle atrophy by NeuroHeal in a pre-clinical model of lumbar root avulsion with delayed reimplantation. Sci. Rep. 7, 12028.
Romeo-Guitart, D., Fores, J., Herrando-Grabulosa, M., Valls, R., Leiva-Rodriguez, T., Galea, E., Gonzalez-Perez, F., Navarro, X., Petegnief, V., Bosch, A., Coma, M., Mas, J.M., Casas, C., 2018. Neuroprotective drug for nerve trauma revealed using artificial intelligence. Sci. Rep. 8, 1879.
Ruven, C., Badea, S.R., Wong, W.M., Wu, W., 2018. Combination treatment with exogenous GDNF and fetal spinal cord cells results in better Motoneuron survival and functional recovery after avulsion injury with delayed root Reimplantation. J. Neuropathol. Exp. Neurol. 77, 325–343.
Sabatier, M.J., To, B.N, Rose, S., Nicolini, J., English, A.W., 2012. Chondroitinase ABC reduces time to muscle reinnervation and improves functional recovery after sciatic nerve transection in rats. J. Neurophysiol. 107, 747–757.
Sakuma, M., Gorski, G., Sheu, S.H., Lee, S., Barrett, L.B., Singh, B., Omura, T., Latremoliere, A., Woolf, C.J., 2016. Lack of motor recovery after prolonged denervation of the neuromuscular junction is not due to regenerative failure. Eur. J. Neurosci. 43, 451–462.
Senger, J.L., Chan, K.M., Macandili, H., Chan, A.W.M., Verge, V.M.K., Jones, K.E., Webber, C.A., 2019. Conditioning electrical stimulation promotes functional nerve regeneration. Exp. Neurol. 315, 60–71.
Shakhbazau, A., Mohanty, C., Shcharbin, D., Bryszewska, M., Caminade, A.M., Majoral, J.P., Alant, J., Midha, R., 2013. Doxycycline-regulated GDNF expression promotes axonal regeneration and functional recovery in transected peripheral nerve. J. Control. Release 172, 841–851.
Shin, A.Y., Spinner, R.J., Steinmann, S.P., Bishop, A.T., 2005. Adult traumatic brachial plexus injuries. J. Am. Acad. Orthop. Surg. 13, 382–396.
Sulaiman, O.A., Gordon, T., 2000. Effects of short- and long-term Schwann cell denervation on peripheral nerve regeneration, myelination, and size. Glia 32, 234–246.
Sulaiman, W., Gordon, T., 2013. Neurobiology of peripheral nerve injury, regeneration, and functional recovery: from bench top research to bedside application. Ochsner J. 13, 100–108.
Sulaiman, O.A.R., Gordon, T., 2018. A rat study of the use of end-to-side peripheral nerve repair as a "babysitting" technique to reduce the deleterious effect of chronic

denervation. J. Neurosurg. 1-11.
Tajdaran, K., Gordon, T., Wood, M.D., Shoichet, M.S., Borschel, G.H., 2016. A glial cell line-derived neurotrophic factor delivery system enhances nerve regeneration across acellular nerve allografts. Acta Biomater. 29, 62–70.
Tetzlaff, W., Alexander, S.W., Miller, F.D., Bisby, M.A., 1991. Response of facial and rubrospinal neurons to axotomy: changes in mRNA expression for cytoskeletal proteins and GAP-43. J. Neurosci. 11, 2528–2544.
Torres-Espin, A., Corona-Quintanilla, D.L., Fores, J., Allodi, I., Gonzalez, F., Udina, E., Navarro, X., 2013. Neuroprotection and axonal regeneration after lumbar ventral root avulsion by re-implantation and mesenchymal stem cells transplant combined therapy. Neurotherapeutics. 10, 354–368.
Tosolini, A.P., Morris, R., 2012. Spatial characterization of the motor neuron columns supplying the rat forelimb. Neuroscience 200, 19–30.
Wang, H., Sorenson, E.J., Spinner, R.J., Windebank, A.J., 2008. Electrophysiologic findings and grip strength after nerve injuries in the rat forelimb. Muscle Nerve 38, 1254–1265.
Wang, T., Zeng, L.N., Zhu, Z., Wang, Y.H., Ding, L., Luo, W.B., Zhang, X.M., He, Z.W., Wu, H.F., 2019. Effect of lentiviral vector-mediated overexpression of hypoxia-inducible factor 1 alpha delivered by pluronic F-127 hydrogel on brachial plexus avulsion in rats. Neural Regen. Res. 14, 1069–1078.
Watabe, K., Ohashi, T., Sakamoto, T., Kawazoe, Y., Takeshima, T., Oyanagi, K., Inoue, K., Eto, Y., Kim, S.U., 2000. Rescue of lesioned adult rat spinal motoneurons by adenoviral gene transfer of glial cell line-derived neurotrophic factor. J. Neurosci. Res. 60, 511–519.
Wong, J.N., Olson, J.L., Morhart, M.J., Chan, K.M., 2015. Electrical stimulation enhances sensory recovery: a randomized controlled trial. Ann. Neurol. 77, 996–1006.
Wu, W., Li, L., Yick, L.W., Chai, H., Xie, Y., Yang, Y., Prevette, D.M., Oppenheim, R.W., 2003. GDNF and BDNF alter the expression of neuronal NOS, c-Jun, and p75 and prevent motoneuron death following spinal root avulsion in adult rats. J.Neurotrauma 20, 603–612.
Yuan, Q., Wu, W., So, K.F., Cheung, A.L., Prevette, D.M., Oppenheim, R.W., 2000. Effects of neurotrophic factors on motoneuron survival following axonal injury in newborn rats. Neuroreport 11, 2237–2241.
Zhou, L.H., Wu, W., 2006. Survival of injured spinal motoneurons in adult rat upon treatment with glial cell line-derived neurotrophic factor at 2 weeks but not at 4 weeks after root avulsion. J.Neurotrauma 23, 920–927.